# Epitaxial Rare Earth Oxide Growth on GaN for Enhancement-mode MOSFETs

J. S. Jur*, V. D. Wheeler*, M. T. Veety**, D. J. Lichtenwalner*, D. W. Barlage**, M. A. L. Johnson*

* Dept. of Materials Science and Engineering, North Carolina State University, Raleigh, NC 27695, USA
** Dept. of Electrical and Computer Engineering, North Carolina State University, Raleigh, NC 27695, USA
*Email: jsjur@ncsu.edu; Phone: (919) 515-6174*

***Keywords:*** High-κ, Rare Earth, Lanthanum Oxide, Scandium Oxide, GaN, MOSFET, Processing, MBE, Gallium Oxide, Passivation

***Abstract***

**Epitaxial growth of rare earth oxides are investigated as gate dielectric materials for GaN-based MOSFET devices. Real-time monitoring of $La_2O_3$ and $Sc_2O_3$ growth by MBE shows different growth progression of the epitaxial oxides. XPS analysis provides further detail about the growth of the oxides. Electrical results show a >10x decrease in leakage current density for a 50 Å $La_2O_3$ epitaxial dielectric as compared to a significantly thicker (600 Å) $Si_3N_4$ dielectric on GaN, despite the high lattice mismatch between the $La_2O_3$ and GaN (21%). The performance enhancement is believed to be due in part to a native $Ga_2O_3$ passivation of the GaN during the initial stage of the epitaxial oxide growth.**

***Introduction***

GaN based enhancement-mode metal oxide semiconductor field effect transistor (MOSFET) devices ($n_s > 4x10^{13}$ $cm^{-2}$) as that shown in **Figure 1**, have been identified for high-power and high-frequency device applications **[1].** This MOSFET design is ideal as it is consistent with corresponding Si-based devices that have shown to be efficiently scaled. Early investigations into such devices were based on III-V materials such as GaAs **[2]**. Molecular beam epitaxy (MBE) growth of dielectrics on GaAs has yielded enhancement-mode devices. However, the use of GaAs is limited by the oxidation of GaAs: $2GaAs + 3O_2 \rightarrow Ga_2O_3[s] + As_2O_3[s]$ **[3]**. Fermi-level pinning interface states are formed as a result of the competing condensed phase reactions. For GaN, the oxidation of nitrogen results in a volatile nitrous oxide, thereby eliminating this potential source of Fermi level pinning states. A number of high-κ gate oxides have been examined for use in GaN MOSFETS including $Sc_2O_3$ **[4]**, $Gd_2O_3$ **[5]**, and $HfO_2$ **[6]**. Still, their application in MOSFET devices is limited by parasitic resistance between the gate and GaN, reducing the attainable breakdown voltage. In general, it is optimal to use a high-κ dielectric with a combination of high permittivity (ε > GaN) and high band gap energy ($E_G$ > GaN) in order to sufficiently reduce the leakage current density **[7]**. These properties are characteristic of the rare earth oxides (Sc-Lu; La-Yb). In addition, the lighter rare earth oxides are hexagonal in structure. This offers the potential for epitaxial growth on hexagonal GaN, a condition that is optimal to reduce leakage caused by defects. However, this leakage reduction can be quickly lost due to high lattice mismatch with GaN, creating leakage paths via growth dislocations **[5].** In this work, the epitaxial growth of $La_2O_3$ (ε = 20-28, $E_G$ = 5.6 eV) and $Sc_2O_3$ (ε = 13-14, $E_G$ = 6 eV) on GaN is investigated as a means to yield high performance enhancement-mode MOSFET devices.

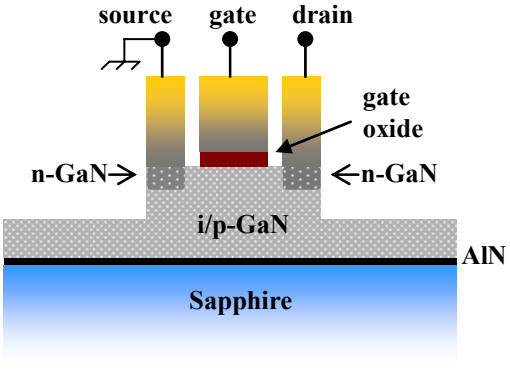


**Figure 1**. Enhancement-mode GaN MOSFET with source/drain selective area regrowth.

***Experimental***

For the rare earth oxide growth study, 1 µm intrinsic hexagonal phase GaN was prepared by metal-organic chemical vapor deposition on 50 mm diameter c-plane sapphire substrates. The surface of the GaN was treated by a $K_2(SO_4)_2$ acid dip followed by a DI water rinse prior to oxide deposition. $La_2O_3$ and $Sc_2O_3$ oxide films (15-50 Å) were deposited using thermal evaporation of elemental high purity La (1700 °C) and Sc (1230 °C) in a ultra-high vacuum SVT Associates MBE system ($P_{background}$ = $5x10^{-10}$ Torr). A GaN substrate temperature of 400 °C was used during

oxide growth, which is below the thermal limit for a 2x1 GaN surface reconstruction. Ultra-high purity oxygen was delivered to the growth chamber to provide an oxygen partial pressure of $5x10^{-7}$ Torr as monitored by an ion gauge. The deposition rates of $La_2O_3$ (1.4 Å /min) and $Sc_2O_3$ (3.5Å/min) was monitored with a quartz crystal monitor prior to exposure to the GaN substrate. *In situ* analysis of oxide growth was conducted with reflection high energy electron diffraction (RHEED) analysis. After growth of the oxide, the oxygen flux was discontinued and the substrate temperature was held at 400 °C for an additional 10 minutes.

X-ray photoelectron spectrospcopy (XPS) characterization of the oxide films was performed using a Riber LAS3000 analytical system equipped with a two stage cylindrical mirror-style analyzer. Spectra was acquired with a Mg Kα (1253.6 eV) non-monochromatic x-ray source, a take off angle of 75° from surface, and a 0.1 eV step size. The C-1s binding energy (285.0 eV) was used as the offset reference. The chemical bonding states of the O-1s and Ga-$2p_{3/2}$ were evaluated using a CASA XPS peak fitting program. BF-STEM analysis of the oxide film on GaN was conducted using a Hitachi S-5500 SEM with 0.4 nm resolution at 30 kV. Cross sectional samples were prepared using a FEI Quanta 200 3D focused ion beam system.

***Results and Discussion***

The growth of $La_2O_3$ and $Sc_2O_3$ films on hexagonal-GaN were examined. Prior to the growth of the oxide, the GaN was treated in an acid solution to yield a Ga-face that promotes the formation of a thin $Ga_2O_3$ native oxide. RHEED analysis of the GaN surface shown in **Figure 2 (a)** represents the [01-10]/[120] lattice plane of hexagonal GaN. At a 30° rotation, the [11-20]/[110] lattice plane is also observed. The spacing of the [01-10]/[120] lattice plane RHEED pattern provides detail on the planar lattice spacing on the surface of the analyzed sample. The RHEED is calibrated with a Si(001) standard, giving a GaN lattice parameter (*a*) of 3.19 Å (bulk GaN = 3.189 Å). The RHEED pattern for 50 Å $La_2O_3$ grown on GaN is provided in **Figure 2 (b)**. The pattern is representative of an epitaxial $La_2O_3$ film that is hexagonal in structure with an *a* lattice parameter of 3.90 Å (*a* = 3.826 Å for bulk hexagonal-$La_2O_3$), yielding a 21% lattice mismatch between substrate and oxide film. A hexagonal structure is expected for the $La_2O_3$ at the growth conditions used. The spot-like appearance of the diffraction streaks is indicative

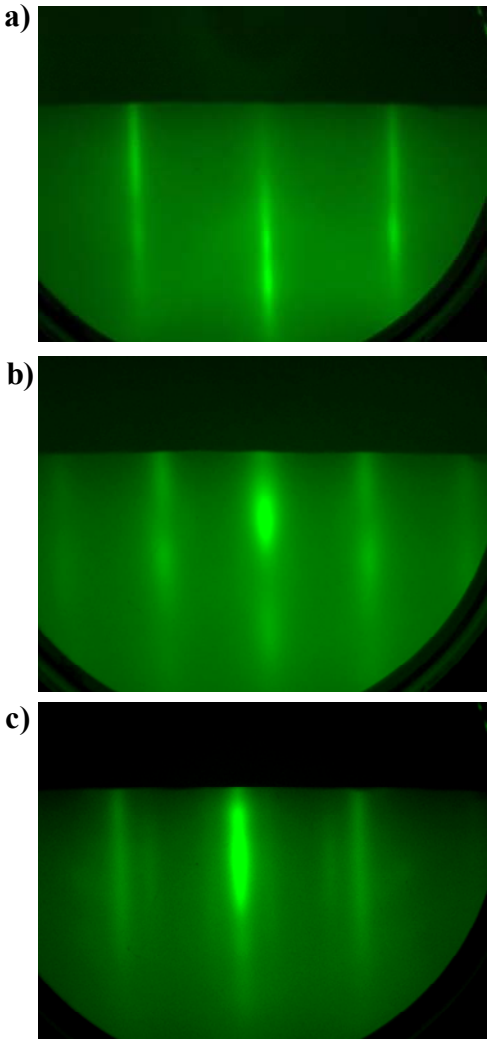


**Figure 2**. RHEED patterns of (a) the [01-10]/[120] surface of GaN prior to deposition and after 50 Å (b) $La_2O_3$ and (c) $Sc_2O_3$.

of non-surface (i.e. 3D) diffraction as a result of a rough film surface.

In **Figure 2 (c)** an epitaxial RHEED pattern is also obtained for 50 Å $Sc_2O_3$ growth on GaN (*a* = 3.19 Å). Again a hexagonal structure of the rare earth oxide is observed. However, a surface reconstruction (the additional diffraction streaks) in the oxide film indicates a 2D superstructure and thus a smooth 2D film morphology. An *a* lattice parameter of 3.42 Å for the $Sc_2O_3$ yields a lattice mismatch of 7.2% with the GaN substrate.

**Figure 3** shows a time-elapsed cross sectional line scan from the RHEED pattern, beginning with the GaN pattern and ending with the $La_2O_3$ 10 minutes after the oxygen partial pressure has been reduced. Upon $La_2O_3$ deposition, an incubation time is observed prior to

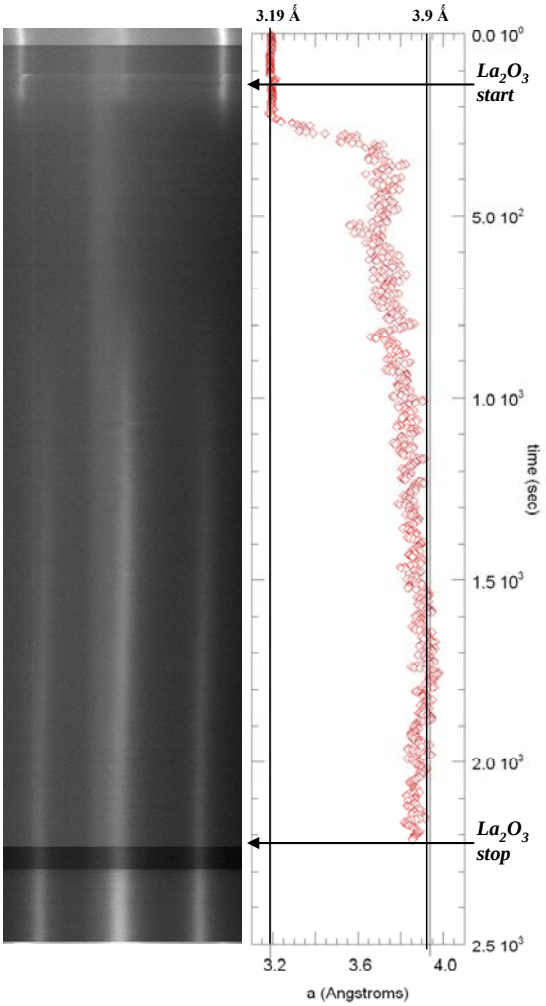


**Figure 3.** Line scan of RHEED pattern during epitaxial growth of 50 Å $La_2O_3$ with corresponding change in lattice parameter.

the appearance of the epitaxial nature of the $La_2O_3$ thin film. A time-elapsed line scan of the $Sc_2O_3$ RHEED pattern (not provided) shows a abbreviated incubation period as compared to the $La_2O_3$ growth. In addition < 0.5% reordering occurs after the $Sc_2O_3$ growth is ceased and the oxygen flux is reduced.

For heteroepitaxial film growth, the lattice mismatch between the substrate and film can have a significant effect on the nucleation and growth modes of the film **[8]**. A quasi-zero lattice matching results in a Frank-Van der Merwe growth, described as layer-by-layer growth. The observation of a negligible incubation time period, 2D superstructure, and low misfit all suggest a layer-by layer growth mode for $Sc_2O_3$ on GaN in the conditions of the experiment. An increase in the misfit (the $La_2O_3$ case) results in a 3D character of the film growth, referred to as Volmer-Weber growth (island) or Stranski-Krastonov growth (layer then island). The loss of the GaN RHEED pattern altogether at the start of the $La_2O_3$ growth is suggestive that $La_2O_3$ has completely covered the GaN surface. Strain relief then results in the island formation, a process that would be appropriately described by Stranski-Krastonov growth.

XPS was performed as a method to further investigate the growth modes of the epitaxial oxides. After 50 Å of $La_2O_3$, the Ga-$2p_{3/2}$ peak from the GaN substrate is still observed. For a similar thickness of $Sc_2O_3$, there is no observation of a Ga-$2p_{3/2}$ peak. This would confirm the layer-by layer growth of the $Sc_2O_3$ and the island growth for $La_2O_3$. However, it is noted that the $La_2O_3$ has a high affinity for hydroxide formation when exposed to atmosphere **[9]**, as is the case in performing *ex situ* XPS in this study. $Sc_2O_3$ does not have the same propensity. Evidence for the hydroxide formation is observed in the O-1s XPS spectra by the high intensity of the La-O-H peak at a binding energy of 532.3 eV. As a result agglomerates of $La(OH)_3$ are formed on the surface, potentially leading to an exposed GaN interface. *In situ* capping of the $La_2O_3$ with a barrier metal can prevent hydroxide formation. BF-STEM imaging shown in **Figure 4** of the 50 Å $La_2O_3$ with a 200 Å *in situ* capping layer of Ta does show a smooth layer of $La_2O_3$ deposited on the surface of the GaN and is a suitable prevention of the hydroxide formation.

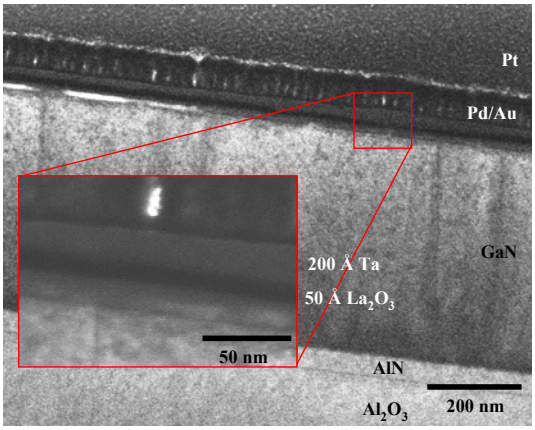


**Figure 4.** BF-STEM cross sectional imaging of Ta/$La_2O_3$ gate stack deposited on GaN.

From the XPS analysis of $La_2O_3$ growth on GaN, a Ga-O peak is observed in both the O-1s and Ga-2p3/2 spectra, suggesting the presence of a thin $Ga_2O_3$ native oxide. XPS analysis of the GaN substrate after acid treatment shows the propensity for the native oxide formation of the Ga-terminated GaN. A thin native oxide would

be expected by way of the DI water rinse following the acid treatment or exposure to atmosphere.

The leakage current density of a mesa-isolated MOSFET device structure gate stack consisting of 50 Å $La_2O_3$ on Ga-terminated GaN is shown in **Figure 5**. An *in situ* cap of Ta (200 Å) was used to prevent hydroxide formation. For comparison, a similar device structure with a 600 Å $Si_3N_4$ dielectric layer is also provided. It is observed that $La_2O_3$ device has a >10x improvement over the significantly thicker $Si_3N_4$ dielectric. Considering the observation of the high lattice mismatch during the $La_2O_3$ growth, a high density of defects is expected which would be a route for increased gate leakage. A possible route for reduced effect of these defects is the surface passivation of the GaN. In this way, controlled native oxide growth on GaN potentially could be used as psuedomorphic transition layer allowing for either a reduction in defects prior to the deposition, or as a barrier to leakage paths between defects in the oxide to the GaN.

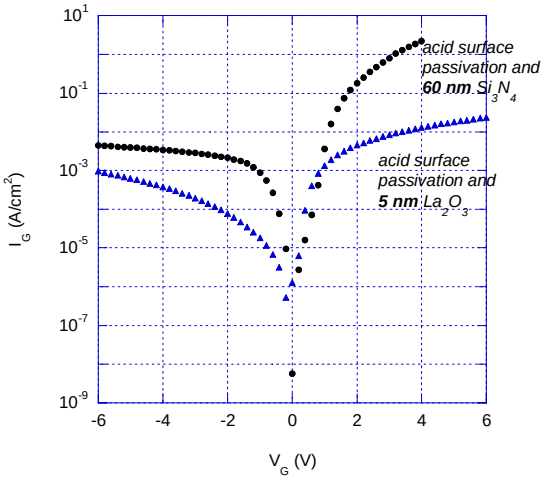


**Figure 5.** Leakage current density comparison of 50 Å $La_2O_3$ and 600 Å $Si_3N_4$ deposited on Ga-terminated GaN.

## *Conclusions*

Epitaxial growth mechanisms of the $La_2O_3$ and $Sc_2O_3$ on Ga-terminated GaN have been examined, for their potential use in enhancement-mode GaN MOSFET devices. Evidence for opposing growth modes have been observed, which suggest limitations on the lower limit thickness optimization (i.e. scaling) of such devices. Despite the high lattice mismatch for the $La_2O_3$, an epitaxial film of 50 Å thickness is observed to have >10x improvement in gate leakage current as compared to a >10x thicker $Si_3N_4$ dielectric. The decreased leakage is believed to be due in part to a promoted native oxide formation on the GaN.


## *Acknowledgements*

The authors would like to thank M. Morgensen for conducting the electrical measurements. The authors of this paper were funded by a Defense Advanced Research Projects Agency Young Investigators Award.


## *References*


1. Matocha, K., T.P. Chow, and G. R.J., *High-voltage normally off GaN MOSFETs on sapphire substrates.* IEEE Transaction on Electron Devices, 2005. **52**(1).
2. Ren, F., et al., *Demonstration of enhancement-mode p- and b-channel GaAs MOSFETs with $Ga_2O_3(Gd_2O_3)$ as gate oxide.* Solid-State Electronics, 1997. **41**(11): p. 1751-1753.
3. Schwartz, G., *Analysis of native oxide-films and oxide substrate reactions on III-V semiconductors using thermochemical phase-diagrams.* Thin Solid Films, 1983. **103**(1-2): p. 3-16.
4. Cho, H., et al., *Influence of gate oxide thickness on $Sc_2O_3$/GaN MOSFETs.* Solid-State Electronics, 2003. **47**(10): p. 1757-1761.
5. Johnson, J., et al., *$Gd_2O_3$/GaN metal-oxide-semiconductor field-effect transistor.* Applied Physics Letters, 2000. **77**(20): p. 3230-3232.
6. Chang, Y., et al., *Structural and electrical characteristics of atomic layer deposited high kappa $HfO_2$ on GaN.* Applied Physics Letters, 2007. **90**(23)
7. Robertson, J. and B. Falabretti, *Band offsets of high K gate oxides on III-V semiconductors.* Journal of Applied Physics, 2006. **100**(1): p. -.
8. Scheel, H.J. and T. Fukuda, *Crystal Growth Technology*. 1 ed. 2003, Chichester, West Sussex, England: John Wiley and Sons.
9. Gougousi, T., M.J. Kelly, and G.N. Parsons, *The role of the OH species in high-k/polycrystalline silicon gate electrode interface reactions.* Applied Physics Letters, 2002. **80**(23): p. 4419-4421.


## *List of Acronyms*

MOSFET: metal-oxide-semiconductor field effect transistor
$n_s$: sheet charge
MBE: molecular beam epitaxy
XPS: x-ray photoelectron spectroscopy
RHEED: reflection high energy electron diffraction
BF-STEM: bright field – scanning transmission electron microscopy
SEM: scanning electron microscopy